JCTC Journal of Chemical Theory and Computation

Article

pubs.acs.org/JCTC

Long-Range Corrected DFT Meets *GW*: Vibrationally Resolved Photoelectron Spectra from First Principles

Lukas Gallandi and Thomas Körzdörfer*

Institut für Chemie, Universität Potsdam, Karl-Liebknecht-Straße 24-25, 14476 Potsdam, Germany

Supporting Information

ABSTRACT: We propose an entirely nonempirical and computationally efficient scheme to calculate highly reliable vibrationally resolved photoelectron spectra for molecules from first principles. To this end, we combine nonempirically tuned long-range corrected hybrid functionals with non-self-consistent many-body perturbation theory in the G_0W_0 approximation and a Franck−Condon multimode analysis based on DFT-calculated frequencies. The vibrational analysis allows for a direct comparison of the *GW*-calculated spectra to gas-phase ultraviolet photoelectron measurements of neutral and anionic molecules, respectively. Direct comparison of the calculated peak maxima with experiment yields mean absolute errors below 0.1 eV for ionization potentials, electron affinities, and fundamental gaps, clearly outperforming commonly used G_0W_0 approaches at similar numerical costs.

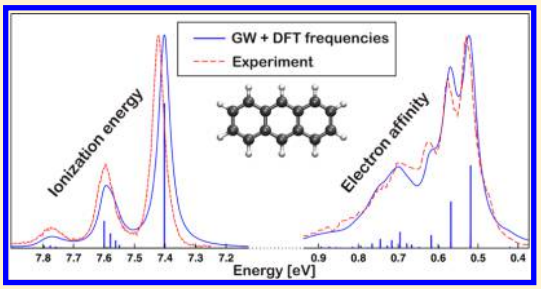

1. INTRODUCTION

The determination of highly accurate ionization potentials (IPs), electron affinities (EAs), and fundamental gaps of organic and inorganic materials and the alignment of these energy levels at the interface of two materials have been a long-standing challenge for both theory and experiment in materials science. This is particularly true for applications in photovoltaics and molecular electronics, where the energetics of the creation and transport of charged excitations are key factors determining the functionality and efficiency of devices. While the theoretical prediction of very accurate IPs and gaps from highly accurate wave function methods is limited to finite systems with only a few electrons, the state of the art for the calculation of charged excitation energies and fundamental gaps of large molecules, clusters, and periodic solids is many-body perturbation theory in the *GW* approximation.[1] Here, *G* is the noninteracting Green's function and *W* is the screened Coulomb interaction between quasiparticles, i.e., electrons or holes with their polarization cloud.

Owing to the high computational cost of fully or partially self-consistent *GW* calculations, most applications of the *GW* method employ a non-self-consistent implementation, hereafter referred to as G_0W_0.[2] In this case, *G* and *W* are constructed from orbitals and eigenvalues obtained from a mean field approach such as density functional theory (DFT)[3,4] or the Hartree−Fock (HF) method. As a consequence, the quality of the results obtained from G_0W_0 is sensitive to the used starting point.[5−11] This is demonstrated in Figure 1 for the case of the DNA/RNA nucleobases, where we compare various G_0W_0 starting points (denoted as G_0W_0@method) with experimental and theoretical reference data.[8,12,13] Using a standard semilocal DFT functional, such as the one of Perdew, Burke, and Ernzerhof (PBE),[14] as a starting point typically leads to a significant underestimation of the ionization energy. In contrast, starting the G_0W_0 calculations from HF causes an overestimation of the IPs as compared to the reference data.

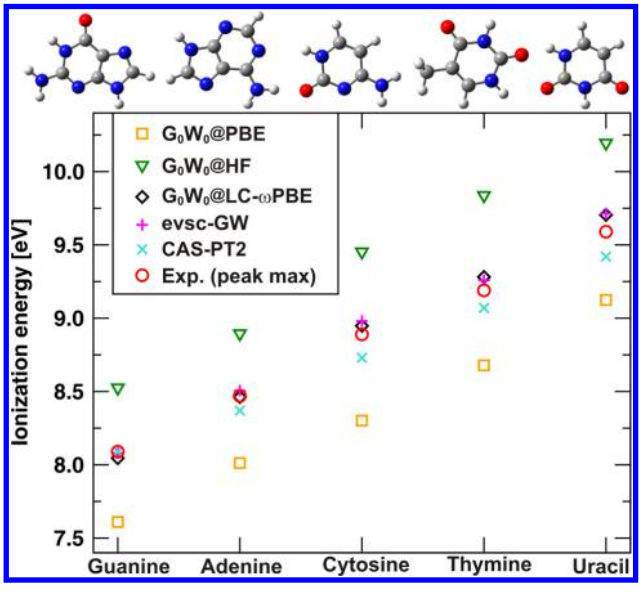

Figure 1. Vertical ionization energies of the DNA/RNA nucleobases guanine (G), adenine (A), cytosine (C), thymine (T), and uracil (U) calculated from G_0W_0@PBE (yellow-orange □), G_0W_0@HF (green ▽), G_0W_0@LC-ωPBE (black ◊), and ev-sc*GW* (pink +). Quantum chemical results obtained from CAS-PT2[12] (light-blue ×) as well as the positions of the peak maxima of experimental photoelectron spectra[13,15] (red ○) are provided as a reference.

Received: August 26, 2015
Published: October 5, 2015

DOI: 10.1021/acs.jctc.5b00820
J. Chem. Theory Comput. 2015, 11, 5391−5400

For the nucleobases studied here, the difference between IPs obtained from G_0W_0@PBE and G_0W_0@HF is about 1 eV. Most importantly, neither G_0W_0@PBE nor G_0W_0@HF yield satisfactory agreement with the experimental and theoretical reference data.

This failure of the most commonly employed starting points can be explained by the fact that the quasiparticle energies calculated from G_0W_0 are heavily influenced by the screening of the Coulomb interaction, which is basically determined by the eigenvalue gap predicted by the underlying electronic structure theory. Semilocal DFT approaches, such as PBE, yield a Kohn−Sham (KS) eigenvalue gap that is severely underestimated, thus leading to significant overscreening. In contrast, the HF approach leads to an underscreening due to its too large eigenvalue gap. Using hybrid functional starting points typically improves the accuracy of G_0W_0 quasiparticle energies,[9,16] and nonempirical tuning procedures for determining the optimal fraction of HF exchange have been suggested.[11,17] However, while the fraction of HF exchange needed to obtain optimal quasiparticle energies for the frontier orbitals is typically close to or above 70%,[17] the optimal value for the prediction of full spectra is much smaller.[11] In a recent benchmark, two variants of the range-separated hybrid functional CAM-B3LYP have been employed as starting points for G_0W_0 calculations, yielding surprisingly accurate results.[16]

A different work-around for this problem with non-self-consistent G_0W_0 that does not involve the high computational costs of fully self-consistent GW[10,18−20] is to aim for self-consistency only in the quasiparticle eigenvalues.[2,8,21] Although the eigenvalue-self-consistent GW (ev-scGW) approach is not optimal for predicting full quasiparticle spectra,[9] it improves the obtained IPs significantly, as can be seen from the DNA/RNA nucleobases depicted in Figure 1. However, ev-scGW is also more expensive than G_0W_0, and, just like the latter, it can fail in situations for which the reference density of the starting point (and not only the eigenvalue gap) is wrong. This can happen, for example, in molecular donor−acceptor systems, where semilocal DFT predicts a spurious charge transfer between the two molecules. In such situations, ev-scGW calculations based on a wrong DFT reference are doomed to fail in predicting a correct level alignment.[22]

In this article, we propose a novel method that predicts highly accurate and vibrationally resolved photoelectron spectra from first principles at the numerical costs of a G_0W_0 calculation. The basic idea is to employ a DFT starting point in which the HOMO/LUMO gap, that is, the energy difference between the highest occupied (HOMO) and the lowest unoccupied molecular orbital (LUMO), is already a reasonable approximation to the molecules' fundamental gap, that is, the energy difference between the IP and EA. This is achieved by using a long-range corrected (LC) hybrid functional in which the range-separation parameter is nonempirically tuned to match the IP theorem.[23] To allow for a direct comparison between the vertical IPs and EAs from the GW method to the experimentally determined peak maxima of photoelectron spectra of the neutral or anionic molecules, respectively, we perform a full Franck−Condon (FC) multimode analysis based on DFT frequencies. By comparison to experimental reference data, it is demonstrated that the IP-tuned LC-hybrid functional significantly improves upon commonly used starting points for G_0W_0 at similar computational costs. By direct comparison to gas-phase ultraviolet photoelectron spectroscopy (UPS) data, we find mean absolute errors of less than 0.1 eV for the determination of IPs, EAs, and fundamental gaps, which is at the limit of what can be expected from using the GW approximation.

2. METHODOLOGY

By virtue of the IP theorem, the HOMO eigenvalue of exact generalized Kohn−Sham (GKS) theory equals the system's vertical IP, i.e., the total energy difference between the neutral and cationic system for a fixed geometry. Standard semilocal and global hybrid functionals, however, do not obey the IP theorem. It is frequently argued that this failure is related to what is referred to as the self-interaction error[24] (SIE) or localization/delocalization[25,26] error of DFT, and many approaches to reduce SIEs have been suggested.[24,27−33] In a series of recent papers by several groups, the concept of long-range corrected hybrid functionals, in which the range-separation parameter is nonempirically tuned to match the IP theorem, was successfully applied to reduce SIEs in the DFT description of molecules.[23,34−56] In particular, the HOMO and LUMO eigenvalues obtained from this class of functionals have been demonstrated to be good approximations to IP and EAs, respectively,[35−37,39,56] which suggests that tuned LC hybrids lend themselves as favorable starting points for G_0W_0. In a way, using these functionals as a starting point for G_0W_0 can be interpreted as generating a quasi-self-consistency in the eigenvalues of the frontier orbitals. In fact, it has been argued that not only the HOMO/LUMO gaps but also the valence eigenvalue spectra obtained from tuned LC-hybrids can be reasonable approximations to quasiparticle energies.[42,45,57] However, since the LC-hybrid calculation is carried out self-consistently, a G_0W_0 approach based on such a starting point has the potential to go beyond ev-scGW in those situations where standard semilocal functionals fail to predict a correct ground-state density.

The central premise underlying all LC functionals is the separation of the Coulomb operator into short- and long-range components using the standard error function

$$\frac{1}{r} = \underbrace{\frac{1-\mathrm{erf}(\omega r)}{r}}_{\mathrm{SR}} + \underbrace{\frac{\mathrm{erf}(\omega r)}{r}}_{\mathrm{LR}} \tag{1}$$

This ansatz allows the combination of the semilocal or global hybrid description of short-range (SR) interactions with the correct asymptotics of full Hartree−Fock exchange in the long range (LR). Here, we employ the LC-hybrid functional LC-ωPBE,[58,59] which combines the short-range ωPBE functional[60,61] with long-range HF exchange and semilocal PBE correlation,[14] i.e.

$$E_{\mathrm{xc}}^{\mathrm{LC}-\omega\mathrm{PBE}} = E_{\mathrm{x}}^{\omega\mathrm{PBE,SR}} + E_{\mathrm{x}}^{\mathrm{HF,LR}} + E_{\mathrm{c}}^{\mathrm{PBE}} \tag{2}$$

Unsurprisingly, the results obtained by LC-ωPBE and other LC hybrid functionals are rather sensitive on the range-separation parameter ω, which is why it was suggested to nonempirically tune ω to obey the IP theorem for each system individually.[23,34,35] This IP-tuning procedure reduces the SIE significantly and yields HOMO/LUMO eigenvalues and gaps that are in very good agreement to theoretical and experimental reference data.[35−37,39,56] In practice, the IP tuning is done by finding the ω that minimizes the difference between the HOMO eigenvalue and the total energy difference between the electronic ground states of the neutral (N electrons) and cationic ($N-1$ electrons) molecules at a fixed geometry, i.e.

DOI: 10.1021/acs.jctc.5b00820
J. Chem. Theory Comput. 2015, 11, 5391−5400

$$\Delta_{IP} = |-\epsilon^{\omega}_{HOMO} - [E_{gs}(\omega,N) - E_{gs}(\omega, N-1)]| \quad (3)$$

The IP-tuning procedure is completely nonempirical and typically converges within only a few self-consistent field (SCF) cycles when using simple linear interpolation. Although it requires a number of SCF calculations for the neutral and cationic molecules of interest, the additional numerical costs introduced by the IP-tuning procedure are not significant compared to the subsequent G_0W_0 calculation. This is because IP tuning includes only occupied states and total energies and, hence, can be carried out using a much smaller basis set than what is typically required to converge a G_0W_0 calculation.

Here, we focus on using IP-tuned LC-ωPBE as a starting point for G_0W_0, hereafter referred to as G_0W_0@LC-ωPBE. Figure 1 shows the results obtained for the DNA/RNA nucleobases. G_0W_0@LC-ωPBE clearly outperforms the standard PBE and HF starting points, yielding a much better agreement to both the theoretical and experimental reference data. In fact, the IPs obtained from G_0W_0@LC-ωPBE are nearly indistinguishable from those obtained from ev-sc*GW*, clearly supporting the assumption that using an IP-tuned LC hybrid starting point amounts to generating a quasi-self-consistency in the eigenvalues and, thus, improving the description of the Coulomb screening.

Figure 1 demonstrates that G_0W_0@LC-ωPBE is a very promising approach for the calculation of quasiparticle energies from first principles without the need for self-consistency or empiricism. However, on the basis of these results, it is very difficult to conclude *how* accurate the G_0W_0@LC-ωPBE predicted IPs are indeed. Comparison to the vertical IPs obtained from the theoretical wave function calculations[12] suggests a small overestimation by as much as 0.1 to 0.2 eV. However, although basis-set extrapolation techniques exist for wave function methods but not for *GW*, they are even more challenging to converge in terms of the basis set than *GW* calculations. In addition, the results of CAS-PT2 calculations can depend on the choice of the active space. Given the fact that both CAS-PT2 and G_0W_0@LC-ωPBE use different approximations, it is hard to say per se which of the methods is more reliable in this particular case. Besides, the comparison to the experimental results is also not straightforward. The experimental IPs shown in Figure 1 were derived from the maxima of the (vibrationally broadened) first ionization peaks seen in ultraviolet photoelectron spectroscopy (UPS) measurements.[13] A straightforward comparison of the vertical ionization energies derived from the theoretical calculations with these numbers could be misleading. In fact, we find that the zero-point vibrational energy correction, the relaxation energy, and vibrational broadening can add up to a difference between vertical IPs and peak maxima of a few tenths of an electron volt. Hence, to allow for a direct comparison of the calculated vertical IPs with the experimentally measured peak maxima, it is necessary to derive the full vibrational structure of the UPS peak from first principles.

To this end, we apply a FC multimode analysis based on the DFT-calculated geometries and vibrational frequencies.[62] In this method, the relative intensity of a multidimensional vibrational transition involving p vibrational modes is obtained as a product of one-dimensional FC integrals, i.e.

$$I(m_1, m_2, ..., m_p, n_1, n_2, ..., n_p) = \prod_{i=1}^{p} \mathrm{FCI}(m_i,n_i)^2 \exp\left\{\frac{-\hbar m_i \nu_i}{k_B T}\right\} \quad (4)$$

where m_i and n_i are the initial and final quantum numbers of the vibrational mode i with frequency ν_i, k_B is the Boltzmann constant, and T is the temperature. In this framework, the shape of the ionization band is governed by the FC integrals $\mathrm{FCI}(m,n) = \langle \Phi_m(\mathbf{Q}_1)|\Phi_n(\mathbf{Q}_2)\rangle$, where $\Phi_m(\mathbf{Q}_1)$ and $\Phi_n(\mathbf{Q}_2)$ are vibrational wave functions of the neutral and charged electronic states, respectively. The FCI can be calculated directly via

$$\mathrm{FCI}(m,n)^2 = e^{-S} S^{(n-m)} \frac{m!}{n!} [L_m^{(n-m)}(S)]^2 \quad (5)$$

with the Laguerre polynomials $L_n^{\alpha}(x)$ and the Huang–Rhys factor $S = \delta^2 \mu\nu/2\hbar$,[63] where δ is the change in the normal coordinate, μ is the reduced mass, and ν is the vibrational frequency of the normal mode. In harmonic approximation, the relaxation energy λ is then given by

$$\lambda = \sum_{i=1}^{p} \hbar\nu_i S_i = \sum_{i=1}^{p} \frac{k_i}{2} \Delta Q_i^2 \quad (6)$$

where ΔQ_i represents the displacement along normal mode i between the equilibrium positions of the two electronic states of interest, e.g., the neutral and cationic states. Equations 4–6 allow the determination of the Huang–Rhys factors S_i, the relaxation energy λ, and the FC integrals $\mathrm{FCI}(m,n)$ and, hence, the relative intensity of a multimode vibrational transition, given that the geometries of the neutral ($\mathbf{Q}_1$) and charged ($\mathbf{Q}_2$) molecules, the vibrational frequencies ν_i, and the corresponding force constants k_i are known.

For molecules with a large number of vibrational modes, the number of FC integrals that needs to be calculated is huge. This problem is well-known from the calculation of vibrationally resolved optical spectra, and effective strategies to reduce the numerical costs have been proposed.[64−66] While these strategies could be applied for our purposes as well, we here follow a simpler approach in which we consider only those vibrational modes with Huang–Rhys factors above a certain threshold (S_{min}) and where we apply a maximum value N for the sum of all initial and final vibrational quantum numbers, i.e., $\sum_i^p m_i \le N$ and $\sum_i^p n_i \le N$. Then, we increase N and decrease S_{min} until the spectrum converges; typical values are $4 \le N \le 8$ and $10^{-5} \le S_{min} \le 10^{-8}$.

FC multimode analysis and similar approaches have been used successfully to study the vibrational progression of UPS spectra.[62,67−69] To derive the absolute position of the UPS peak, however, the (0−0) transition has typically been fitted empirically to yield the best agreement with experiment. In contrast, we here derive the (0−0) transition directly from the vertical ionization energies obtained from *GW* calculations at the neutral geometries. This is illustrated in Scheme 1, which shows a sketch of the potential energies surfaces relevant for the photo attachment and detachment processes. Given the vertical IP (IP_v) and EA (EA_v) obtained from a G_0W_0 calculation at the geometries of the neutral molecules, the (0−0) transitions can be determined from the relaxation energy λ and the zero-point vibrational frequencies of the neutral (E^n_{ZPV}), cationic (E^c_{ZPV}), and anionic (E^a_{ZPV}) states via

DOI: 10.1021/acs.jctc.5b00820
J. Chem. Theory Comput. 2015, 11, 5391−5400

Scheme 1. Potential Energy Surfaces Relevant for the Photo Detachment (Left) and Attachment (Right) Processes[a]

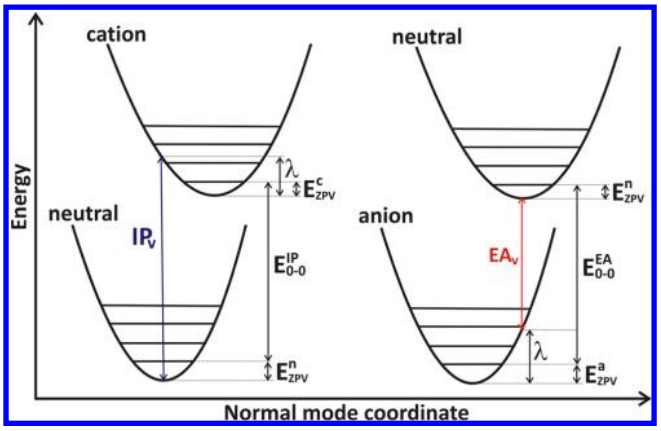

[a]The vertical IP and EA are calculated from G_0W_0 at the neutral geometries using different DFT starting points. The relaxation energy λ and the zero-point vibrational energies are calculated from DFT. From this, the (0−0) transition energies are derived via eqs 7 and 8.

$$E_{0-0}^{\mathrm{IP}} = \mathrm{IP}_{\mathrm{v}} - \lambda - (E_{\mathrm{ZPV}}^{\mathrm{n}} - E_{\mathrm{ZPV}}^{\mathrm{c}}) \quad (7)$$

$$E_{0-0}^{\mathrm{EA}} = \mathrm{EA}_{\mathrm{v}} + \lambda + (E_{\mathrm{ZPV}}^{\mathrm{n}} - E_{\mathrm{ZPV}}^{\mathrm{a}}) \quad (8)$$

The necessary information can be obtained from a DFT-based geometry optimization followed by a vibrational frequency analysis.

In summary, the combination of *GW* calculations for vertical quasiparticle excitation energies with DFT calculations for the geometries, vibrational frequencies, and force constants of the neutral and charged molecules enables us to predict the position of the (0−0) transition and the full vibrational structure of UPS peaks from first principles. This allows us to compare the results of our G_0W_0@LC-ωPBE approach directly to experiment.

3. NUMERICAL APPROACH

All *GW* calculations were performed with the all-electron numerical atom-centered orbital (NAO) code FHIaims using a tier 4 basis set and a very tight grid at the geometries of the neutral molecules.[70−72] We have carefully checked the basis-set and grid convergence with respect to the studied quasiparticle energies. All ev-sc*GW* calculations use a converged PBE calculation as a starting point. The IP-tuning procedure to determine the optimal value for the range-separation parameter ω was carried out using linear interpolation and a tier 2 basis set, which is sufficiently large for DFT (but not for G_0W_0) calculations. Using a tier 2 basis set reduces the cost of the IP-tuning procedure drastically without significantly affecting the results. Hence, the IP-tuning procedure is less costly than the actual G_0W_0 calculation, although it requires several SCF steps to converge. For comparison, we also included the results of ΔSCF calculations of the IP and EA, i.e., total energy differences between the charged and neutral molecules, using the standard global hybrid functional PBEh.

The geometries of all neutral, cationic, and/or anionic molecules, the respective relaxation energies, unscaled vibrational frequencies, and force constants were calculated using the B3LYP functional[73] and a 6-311G++(d,p) basis, as implemented in the QChem program package.[74] The FC factors for the electron attachment and detachment spectra were derived from a multimode analysis using the parallel mode approximation following eqs 4−6. The thus obtained transition intensities were convoluted with Lorentzian functions with a full width at half-maximum (fwhm) that was chosen to match the experimental resolution. Energies of the (0−0) transitions were calculated from the vertical attachment/detachment energies (obtained from the different *GW* methods) via eqs 7 and 8. More details on the calculations, including the IP-tuned values for ω, the vertical and (0−0) quasiparticle energies, the temperature and peak broadening used for the multimode analysis, relaxation energies, and zero-point vibrational corrections, are provided in the Supporting Information.

4. UPS PEAK MAXIMA FROM FIRST PRINCIPLES

Figure 2 shows the vibrationally resolved UPS spectrum for the HOMO peak of thymine compared to the experimental

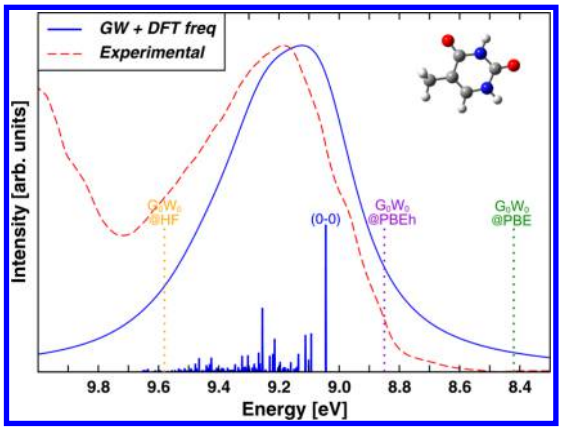

Figure 2. Theoretical prediction of the UPS first ionization peak of thymine at 453 K. The (0−0) energy was calculated from eq 7 using the vertical IP obtained from G_0W_0@LRC-ωPBE; the transition intensities were convoluted with Lorentzian functions of fwhm of 0.25 eV. Experimental spectrum was extracted from ref 13. Dotted lines show the (0−0) transitions as calculated from conventional G_0W_0 calculations.

reference.[13] The (0−0) transition was obtained via eq 7, where the vertical IP was determined by G_0W_0@LC-ωPBE and the relaxation energies and zero-point vibrational frequencies result from DFT. Importantly, the only information from experiment that was used to derive the theoretical spectrum was the temperature of 453 K and the energy resolution given by the experimental setup, which was used to determine the fwhm of the Lorentzian functions. The position of the peak maximum is theoretically predicted to be 9.13 eV, which is 0.06 eV lower in energy than the experimentally determined peak maximum of 9.19 eV.

The same analysis was repeated for all other nucleobases, several G_0W_0 starting points, and ev-sc*GW*. The predicted positions of maxima of the UPS first peak for all DNA/RNA nucleobases and the corresponding mean errors (ME) and mean absolute errors (MAE) for all methods compared to the experiment[13,15] are summarized in Table 1. While G_0W_0@PBE underestimates the IP by 0.65 eV, on average, G_0W_0@HF overestimates the IPs by 0.39 eV. By using the global hybrid functional PBEh[75] (25% HF exchange) as a starting point, the MAE can be reduced to 0.29 eV. Hence, the accuracy of G_0W_0@PBEh is similar to what is found from the calculation of total energy differences (ΔSCF) using the same functional. ev-

DOI: 10.1021/acs.jctc.5b00820
J. Chem. Theory Comput. 2015, 11, 5391−5400

Table 1. Positions of the Maxima of the UPS First Ionization Peak of the DNA/RNA Nucleobases from Experiment and at Different Levels of *GW* Theory and the Respective Mean Errors (ME) and Mean Absolute Errors (MAE)[a]

	exp.	LC-ωPBE	G_0W_0@ LC-ωPBE	G_0W_0@ PBE	G_0W_0@ PBEh	G_0W_0@ HF	ev-sc*GW*	PBEh (ΔSCF)
guanine	8.09[b]	7.96	8.09	7.57	7.87	8.48	8.04	7.80
adenine	8.47[c]	8.28	8.38	7.84	8.14	8.72	8.34	8.09
cytosine	8.89[c]	8.80	8.95	8.19	8.60	9.34	8.86	8.57
thymine	9.19[c]	8.87	9.13	8.43	8.86	9.59	9.01	8.73
uracil	9.59[b]	9.47	9.64	8.97	9.34	10.04	9.56	9.29
ME		−0.17	−0.01	−0.65	−0.29	0.39	−0.09	−0.35
MAE		**0.17**	**0.05**	**0.65**	**0.29**	**0.39**	**0.09**	**0.35**

[a]All values in eV. [b]Ref 15. [c]Ref 13.

sc*GW* and G_0W_0@LC-ωPBE clearly outperform all other methods, both showing an MAE below 0.1 eV.

Comparison of these results to the vertical ionization energies shown in Figure 1 illustrates why it can be problematic to compare the vertical IPs of G_0W_0 directly to experimentally determined peak maxima. The energy difference between the vertical IPs and the peak maxima seen in experiment are different for different molecules, and they can be as large as 0.2−0.3 eV, depending on the zero-point vibrations and relaxation energies of the molecule as well as the temperature and energy resolution of the experiment. As a consequence, the direct comparison of theoretical and experimental data is subject to an intrinsic uncertainty on the order of 0.2−0.3 eV. With the first-principles methods for predicting quasiparticle energies becoming increasingly accurate, this clearly limits our ability to distinguish between the accuracy of different methods. By calculating the full vibrational spectra, we can reduce this uncertainty significantly.

We have now established a methodology that allows for a direct comparison of *GW*-calculated vertical ionization energies to experiment. Also, we have demonstrated that G_0W_0@LC-ωPBE can yield IPs of an accuracy similar to ev-sc*GW* calculations at significantly lower numerical costs. However, Figure 2 illustrates why the DNA/RNA nucleobases are, in fact, not ideal candidates for a straightforward comparison of different *GW* approaches. The existing gas-phase UPS spectra of the nucleobases do not have an ideal energy resolution, which clearly aggravates the comparison of the theoretical and experimental data. In addition, with many vibrational modes contributing to the full vibrational spectrum, the position of the peak maximum in the predicted DNA/RNA spectra is strongly influenced by the temperature and the accuracy of the vibrational frequencies and FC factors derived from DFT.

In the following, we will further analyze the accuracy of G_0W_0@LC-ωPBE by looking at the IPs and EAs for a test set of π-conjugated molecules frequently used in organic electronics. In order to obtain trustworthy results and to reduce the influence of possible systematic errors in the DFT calculations of the vibrational broadening, we focus mainly on molecules for which high-resolution gas-phase UPS spectra exist and for which the peak maximum corresponds to the position of the (0−0) transition.

5. IONIZATION ENERGIES

To study the accuracy of different *GW* approaches for the determination of ionization energies, we focus on the following set of molecules: the anhydrides NDCA, NTCDA, PTCDA and the acenes anthracene, tetracene, and pentacene. This set of molecules was chosen because high-resolution gas-phase UPS spectra have been published for all six molecules, and in all cases, the first UPS peaks are dominated by a strong (0−0) transition. Figures 3 and 4 show the comparison of the

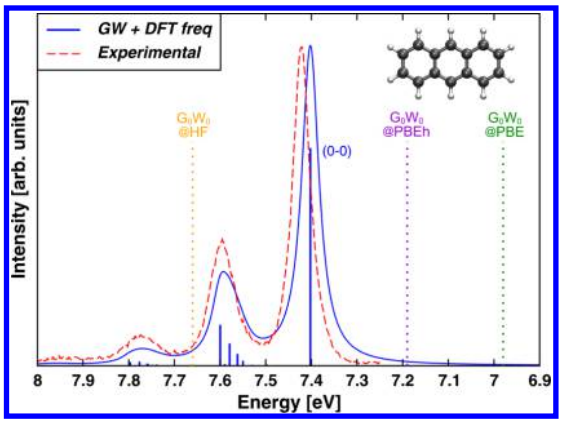

Figure 3. UPS first ionization peak of anthracene at 372 K.[68,76] The (0−0) energy was calculated from eq 7 using the vertical IP obtained from G_0W_0@LRC-ωPBE; the transition intensities were convoluted with Lorentzian functions of fwhm of 0.05 eV.

experimental results with the theoretical calculation based on G_0W_0@LC-ωPBE for anthracene and NTCDA, respectively. The positions of the (0−0) transitions predicted by G_0W_0@PBE, G_0W_0@PBEh, and G_0W_0@HF are indicated by the dotted vertical lines for comparison. The general validity of the FC multimode analysis is supported by the overall excellent

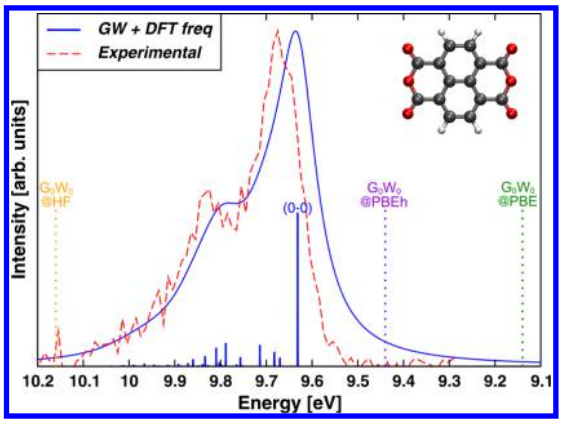

Figure 4. UPS first ionization peak of NTCDA at 493 K.[77,78] The (0−0) energy was calculated from eq 7 using the vertical IP obtained from G_0W_0@LRC-ωPBE; the transition intensities were convoluted with Lorentzian functions of fwhm of 0.08 eV.

DOI: 10.1021/acs.jctc.5b00820
J. Chem. Theory Comput. 2015, 11, 5391−5400

Table 2. IPs, i.e., Positions of the Maxima of the UPS First Ionization Peak of Organic π-Conjugated Molecules from Experiment and at Different Levels of *GW* Theory and the Respective Mean Errors (ME) and Mean Absolute Errors (MAE)[a]

	exp.	LC-ωPBE	G_0W_0@ LC-ωPBE	G_0W_0@ PBE	G_0W_0@ PBEh	G_0W_0@ HF	ev-sc*GW*	PBEh (ΔSCF)
anthracene	7.42[b]	7.29	7.40	6.98	7.19	7.66	7.35	7.13
tetracene	6.94[b]	6.77	6.89	6.53	6.72	7.15	6.84	6.61
pentacene	6.59[b]	6.40	6.51	6.20	6.39	6.80	6.48	6.24
NDCA	8.98[c]	8.85	8.92	8.46	8.75	9.37	8.89	8.75
NTCDA	9.67[c]	9.55	9.63	9.14	9.44	10.16	9.61	9.47
PTCDA	8.20[c]	8.07	8.13	7.80	8.07	8.73	8.15	8.00
ME		−0.14	−0.05	−0.45	−0.21	0.34	−0.08	−0.27
MAE		**0.14**	**0.05**	**0.45**	**0.21**	**0.34**	**0.08**	**0.27**

[a]All values in eV. Calculated vertical IPs, relaxation energies, and zero-point corrections for all molecules are provided in the Supporting Information. [b]Ref 68. [c]Ref 77.

agreement of the temperature-dependent, vibrationally resolved spectra with experiment.

The results for all molecules and methods are summarized in Table 2. Similar to what was already found for the DNA/RNA nucleobases, ev-sc*GW* and G_0W_0@LC-ωPBE show an MAE below 0.1 eV. Both methods slightly underestimate the IP, as can already be seen from Figures 3 and 4. The fact that both methods yield very similar results supports the interpretation that the IP-tuned LC-hybrid starting point leads to a quasi-consistency in the eigenvalues of the frontier orbitals. The MAEs found for all other methods are significantly larger. While the semilocal and global hybrid starting points lead to a significant underestimation of the IP due to overscreening, a HF starting point underscreens and, thus, overestimates IPs. In summary, we find that using an IP-tuned LC-hybrid functional as a starting point for G_0W_0 allows ionization energies of large, π-conjugated molecules to be predicted with an accuracy comparable to that of ev-sc*GW* and MAEs below 0.1 eV. As a next step, we will analyze the performance of the approach for the prediction of electron affinities.

6. ELECTRON AFFINITIES

EAs of molecules can be determined using different experimental techniques. This has to be taken into account when comparing the results of a theoretical calculation with experiment. Here, we focus on EAs that are determined either by gas-phase UPS on valence anions[79,80,82,83] or gas-phase electron attachment.[81] To allow for a reliable comparison to our theoretical approaches, we again require a good energy resolution and spectra that are dominated by a strong (0−0) transition. Using these criteria, we came up with the following set of molecules: anthracene, tetracene, pentacene, *para*-benzoquinone (*p*-BQ), *ortho*-benzoquinone (*o*-BQ), and nitrobenzene.

Using different *GW* methods, we determine the vertical EA for the geometries of the neutral molecules. The energy of the (0−0) transition is then derived from eq 8, and the full vibrational structure of the UPS spectrum is obtained from the multimode FC analysis. Representative for all molecules, Figures 5 and 6 show the UPS spectra of the valence anions of anthracene and nitrobenzene, where the position of the (0−0) transition has been derived from G_0W_0@LC-ωPBE. Again, the positions of the (0−0) transitions as predicted from G_0W_0@PBE, G_0W_0@PBEh, and G_0W_0@HF are indicated by the dotted vertical lines for comparison. Similar to what was found for the IPs, the EAs derived from G_0W_0@LC-ωPBE are highly accurate approximations to the experimental values. The

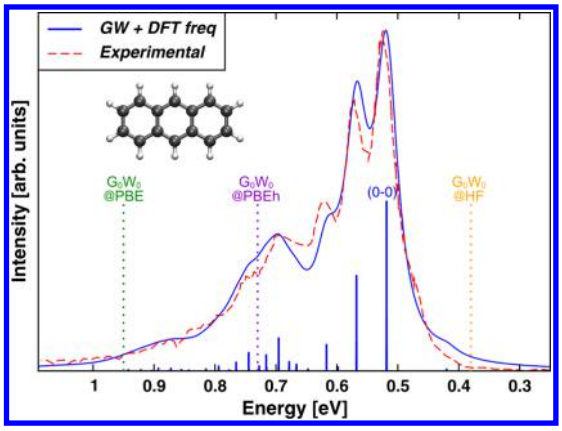

Figure 5. UPS first ionization peak of the anthracene valence anion at 486 K. The (0−0) energy was calculated from eq 8 using the vertical EA obtained from G_0W_0@LRC-ωPBE; the transition intensities were convoluted with Lorentzian functions of fwhm of 0.04 eV. Experimental spectrum was extracted from ref 79.

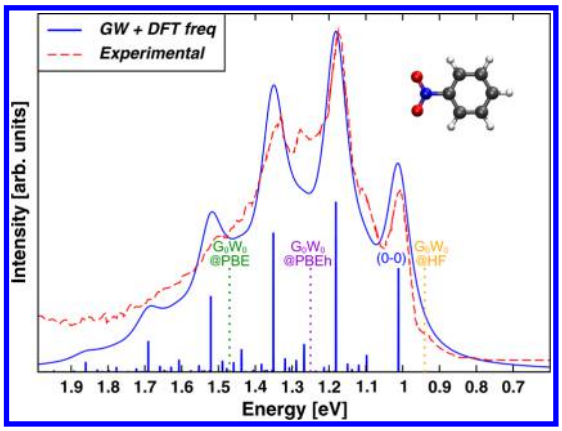

Figure 6. UPS first ionization peak of the nitrobenzene valence anion at 295 K. The (0−0) energy was calculated from eq 8 using the vertical EA obtained from G_0W_0@LRC-ωPBE; transition intensities were convoluted with Lorentzian functions of fwhm of 0.08 eV. Experimental spectrum was extracted from ref 83.

excellent agreement of the theoretical spectra with experiment underlines the validity of the multimode analysis also for the determination of electron affinities.

The results for all molecules and methods are summarized in Table 3. G_0W_0@PBE and G_0W_0@PBEh overestimate the EAs by 0.51 and 0.29 eV, on average, respectively. Interestingly, a

DOI: 10.1021/acs.jctc.5b00820
J. Chem. Theory Comput. 2015, 11, 5391−5400

Table 3. EAs, i.e., Positions of the Maxima of the UPS First Ionization Peak of the Valence Anions of Several Organic π-Conjugated Molecules from Experiment and at Different Levels of *GW* Theory and the Respective Mean Errors (ME) and Mean Absolute Errors (MAE)[a]

	exp.	LC-ωPBE	G_0W_0@ LC-ωPBE	G_0W_0@ PBE	G_0W_0@ PBEh	G_0W_0@ HF	ev-sc*GW*	PBEh (ΔSCF)
anthracene	0.53[b]	0.41	0.52	0.95	0.73	0.38	0.59	0.46
tetracene	1.06[c]	0.96	1.08	1.47	1.27	0.94	1.16	1.03
pentacene	1.39[d]	1.36	1.49	1.86	1.68	1.36	1.58	1.44
p-BQ	1.85[e]	1.79	1.92	2.51	2.28	1.93	2.15	2.10
o-BQ	1.90[e]	2.01	2.04	2.52	2.26	1.92	2.16	2.13
nitrobenzene	1.00[f]	1.02	1.01	1.47	1.25	0.94	1.05	1.04
ME		−0.04	0.05	0.51	0.29	−0.04	0.16	0.08
MAE		**0.07**	**0.05**	**0.51**	**0.29**	**0.08**	**0.16**	**0.11**

[a]All values in eV. Calculated vertical IPs, relaxation energies, and zero-point corrections for all molecules are provided in the Supporting Information. [b]Ref 79. [c]Ref 80. [d]Ref 81. [e]Ref 82. [f]Ref 83.

Table 4. Fundamental Gaps of the Oligo-acenes Derived from the Difference between the Theoretical and Experimental Peak Maxima of the UPS First Ionization Peaks of the Neutral and Anionic Molecules, Respectively, and Mean Errors (ME) and Mean Absolute Errors (MAE) of the Different Theoretical Approaches

	exp.	LC-ωPBE	G_0W_0@ LC-ωPBE	G_0W_0@ PBE	G_0W_0@ PBEh	G_0W_0@ HF	ev-sc*GW*	PBEh (ΔSCF)
anthracene	6.89	6.88	6.88	6.03	6.46	7.28	6.76	6.66
tetracene	5.88	5.81	5.81	5.06	5.45	6.21	5.68	5.58
pentacene	5.20	5.04	5.02	4.34	4.70	5.44	4.91	4.80
ME		−0.08	−0.08	−0.85	−0.45	0.32	−0.21	−0.31
MAE		**0.08**	**0.08**	**0.85**	**0.45**	**0.32**	**0.21**	**0.31**

simple ΔSCF approach yields very accurate results for the EAs with an MAE of only 0.11 eV. ev-sc*GW* performs similarly well, slightly overestimating the EAs for this test set of molecules by 0.16 eV, on average. The EAs obtained from G_0W_0@HF are more accurate, yielding an MAE of only 0.08 eV. The only G_0W_0 method that performs consistently well for both IPs and EAs is G_0W_0@LC-ωPBE, with an MAE below 0.1 eV. In summary, we find that using an IP-tuned LC-ωPBE as a starting point for G_0W_0 not only predicts the IPs but also the EAs of our set of π-conjugated molecules with high accuracy.

Since the tuning scheme used for the range-separation parameter is solely based on the IP criterion, the good performance of the LC-ωPBE and G_0W_0@LC-ωPBE approaches for EAs might come as a surprise. In fact, however, this finding is in line with several previous publications that have studied the performance of the IP-tuning approach for organic, π-conjugated molecules. By studying outer valence photoelectron spectra, for example, it was demonstrated that the IP-tuning procedure not only corrects the HOMO eigenvalue toward the correct IP but also all other occupied and unoccupied valence energy levels.[42,45,57] Problems may arise for the description of valence orbitals that have a significantly different character than the HOMO, a finding that has been attributed to different self-interaction errors in localized vs delocalized orbitals.[30] For example, in situations where the HOMO is a σ- or *n*-type orbital, IP tuning might, per se, not be able to predict the energy levels for π-type orbitals with the same accuracy and vice versa.[42] For the test set of molecules studied in this work, this is apparently no problem. For the case of outer valence spectra, it was found that an unbalanced description of different types of orbitals can be addressed by including a fraction of HF exchange in the SR part of the functional.[45,57] Alternatively, tuning procedures that not only include the molecule's IP but also its EA have been suggested.[23,37,39] A recent benchmark with respect to theoretical reference data for a test set consisting of 24 organic acceptor molecules, however, demonstrates that the specifics of the tuning procedure used in G_0W_0@LC-ωPBE do not affect the overall accuracy of the approach significantly.[84] In summary, while the overall performance of the IP-tuning procedure for EAs certainly depends on the system under study, our results indicate that IP tuning typically also leads to accurate EAs, in particular, when a G_0W_0 correction is applied to the LC-ωPBE eigenvalues.

When looking at the fundamental gap derived by the different methods (Table 4), one finds that the errors for the IPs and EAs in the commonly used starting points of G_0W_0 add up. For example, G_0W_0@PBE underestimates IPs and overestimates EAs. As a consequence, G_0W_0@PBE underestimates the fundamental gap for the acenes by 0.85 eV, on average. Similarly, G_0W_0@HF overestimates the gap by 0.32 eV, on average, although the EAs predicted by the HF starting point present excellent approximations to experiment. Among all methods, G_0W_0@LC-ωPBE yields the best agreement to the experimental gaps with an MAE below 0.1 eV.

At this point, we have demonstrated that G_0W_0@LC-ωPBE yields excellent results for IPs, EAs, and fundamental gaps of molecules, clearly outperforming commonly used starting points for non-self-consistent G_0W_0 calculations. G_0W_0@LC-ωPBE gives very similar IPs to those of ev-sc*GW* at significantly lower costs. For the EAs and gaps of the molecules studied here, G_0W_0@LC-ωPBE even improves to some extent over ev-sc*GW*. Of course, a systematic study on more molecules and the comparison reliable theoretical reference data for vertical quasiparticle energies is needed to corroborate these findings. While this is an interesting aspect that we will follow in future work, we here want to focus on situations in which the G_0W_0@LC-ωPBE approach has a significant advantage over ev-sc*GW*

DOI: 10.1021/acs.jctc.5b00820
J. Chem. Theory Comput. 2015, 11, 5391−5400

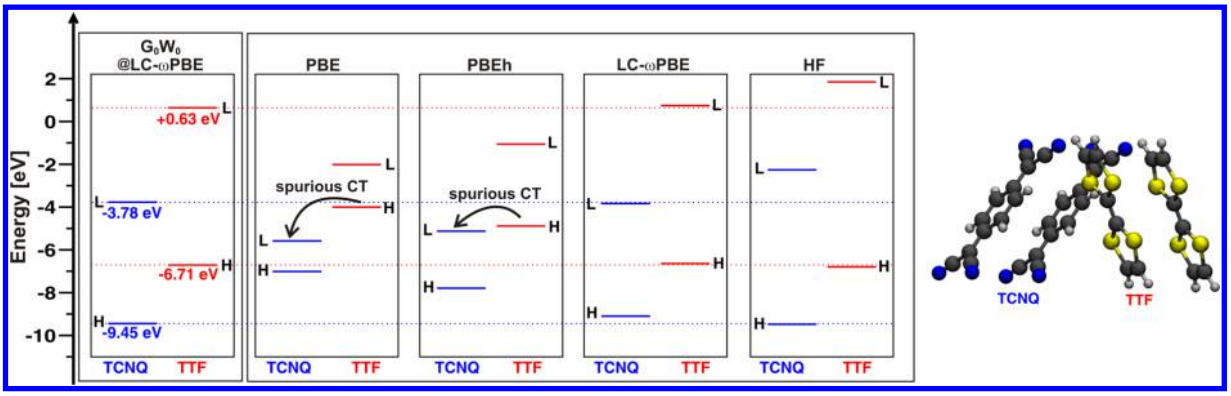

Figure 7. Vertical ionization energies and electron affinities predicted by G_0W_0@LC-ωPBE for the individual TCNQ and TTF molecules (left) compared to the respective HOMO and LUMO eigenvalues predicted by various DFT methods. The HOMO/LUMO gaps predicted by PBE and PBEh are too small, leading to a spurious CT from TTF to TCNQ. This wrong ground-state density affects subsequent G_0W_0 and ev-sc*GW* calculations.

methods, that is, the energy-level alignment in organic donor−acceptor systems.

7. DONOR−ACCEPTOR SYSTEMS

The theoretical description of the energy-level alignment and charge-transfer at organic donor−acceptor interfaces from first principles is a very important but also very challenging problem that has gained a lot of attention in the literature due to its significance in organic electronics.[22,85−88] Generally speaking, the description of charge-transfer processes remains a major challenge to electronic structure theory, which is basically caused by the SIE inherent to commonly used DFT functionals. To illustrate this problem using a prominent example, we here focus on the interface between an important donor material, TTF, and a typical acceptor, TCNQ.[85,87−89]

In the weak-coupling limit, i.e., when the wave function overlap between the donor and acceptor molecules is small, charge transfer between both molecules is dominated by the relative energies of the donor IP and the acceptor EA. Hence, to characterize charge transfer at the organic−organic interface from first principles, it is central to be able to predict as accurate quasiparticle energies as possible. As pointed out above, *GW* is the method of choice for this type of problem. In Figure 7, we show the IPs and EAs for the separate TCNQ and TTF molecules determined from G_0W_0@LC-ωPBE. The IP of TTF is well below the EA of TCNQ. As a consequence, only a negligible charge transfer between the two molecules is expected in the weak-coupling limit. This finding is also confirmed by recently published fully self-consistent *GW* calculations.[22]

Figure 7 reveals a major problem with using standard DFT functionals such as PBE or PBEh for the description of the electronic structure of the TCNQ−TTF interface. It is caused by the fact that semilocal and global hybrid functionals significantly underestimate the HOMO/LUMO gap. As a consequence, the LUMO predicted for TCNQ is, in fact, below the HOMO predicted for TTF. Even in the weak-coupling limit, one therefore observes a significant charge transfer from TTF to TCNQ, which leads to a wrong ground-state density.[22,89] Most importantly, every non-self-consistent *GW* method based on this wrong ground-state density is doomed to fail. As demonstrated in ref 22, the consequences for the prediction of the energy-level alignment predicted from G_0W_0@PBE and G_0W_0@PBEh for donor−acceptor systems such as TTF−TCNQ can be significant. This is also true for the case of ev-sc*GW* if it is based on the wrong ground-state density predicted by semilocal or global hybrid functionals. In contrast to these methods, the HOMO and LUMO eigenvalues predicted by IP-tuned LC-ωPBE are good approximations to the IP and EA, respectively. As a consequence, there is no spurious charge transfer, and the correct ground-state density is predicted. This example illustrates the distinct advantage of using IP-tuned LC-hybrid functionals as a starting point for G_0W_0 as compared to ev-sc*GW* approaches.

8. CONCLUSIONS

We have introduced a first-principles method that allows us to predict highly accurate ionization energies, electron affinities, and fundamental gaps for molecules. This was achieved by combining non-self-consistent *GW* calculations with non-empirically tuned LC-hybrid functionals as a starting point. The full vibrational structure of the corresponding UPS peaks was calculated from a Franck−Condon multimode analysis, thus allowing a systematic comparison of the calculated vertical quasiparticle energies with experiment to be made. Using high-resolution photoelectron spectra for a set of organic π-conjugated molecules as a benchmark, we found that the proposed method shows a mean average error below 0.1 eV for IPs, EAs, and gaps, clearly outperforming standard G_0W_0 approaches at comparable numerical costs. Using the example of the donor−acceptor pair TCNQ/TTF, we stressed that the G_0W_0@LC-ωPBE approach actually goes beyond ev-sc*GW*, as it not only presents a good starting point in terms of the frontier eigenvalues but also in terms of the corresponding orbitals and the ground-state density. Given its numerical efficiency, ease of implementation, general applicability, and high accuracy, the G_0W_0@LC-ωPBE approach presents a valuable alternative to fully or partially self-consistent *GW* methods.

■ ASSOCIATED CONTENT

Supporting Information

The Supporting Information is available free of charge on the ACS Publications website at DOI: 10.1021/acs.jctc.5b00820.

IP-tuned values for ω, vertical and (0−0) quasiparticle energies for all methods, temperatures and peak broadenings used for the multimode analysis, relaxation energies, and zero-point vibrational corrections (PDF)

DOI: 10.1021/acs.jctc.5b00820
J. Chem. Theory Comput. 2015, 11, 5391−5400

AUTHOR INFORMATION

Corresponding Author

*E-mail: koerz@uni-potsdam.de.

Funding

Computer time was provided by the National Energy Research Scientific Computing Center (NERSC), which is supported by the Office of Science of the U.S. Department of Energy under contract DE-AC02-05CH11231.

Notes

The authors declare no competing financial interest.

ACKNOWLEDGMENTS

The authors thank V. Coropceanu, Ch. Ziegler, and S. Lach for providing the experimental UPS data for the acenes and anhydrides as well as N. Marom, P. Rinke, F. Caruso, X. Ren, and V. Blum for helpful discussions.

REFERENCES

(1) Hedin, L. *Phys. Rev.* **1965**, *139*, A796.
(2) Hybertsen, M. S.; Louie, S. G. *Phys. Rev. B: Condens. Matter Mater. Phys.* **1986**, *34*, 5390.
(3) Hohenberg, P.; Kohn, W. *Phys. Rev.* **1964**, *136*, B864.
(4) Kohn, W.; Sham, L. J. *Phys. Rev.* **1965**, *140*, A1133.
(5) Rinke, P.; Qteish, A.; Neugebauer, J.; Freysoldt, C.; Scheffler, M. *New J. Phys.* **2005**, *7*, 126.
(6) Fuchs, F.; Furthmüller, J.; Bechstedt, F.; Shishkin, M.; Kresse, G. *Phys. Rev. B: Condens. Matter Mater. Phys.* **2007**, *76*, 115109.
(7) Marom, N.; Moussa, J. E.; Ren, X.; Tkatchenko, A.; Chelikowsky, J. R. *Phys. Rev. B: Condens. Matter Mater. Phys.* **2011**, *84*, 245115.
(8) Faber, C.; Attaccalite, C.; Olevano, V.; Runge, E.; Blase, X. *Phys. Rev. B: Condens. Matter Mater. Phys.* **2011**, *83*, 115123.
(9) Marom, N.; Caruso, F.; Ren, X.; Hofmann, O. T.; Körzdörfer, T.; Chelikowsky, J. R.; Rubio, A.; Scheffler, M.; Rinke, P. *Phys. Rev. B: Condens. Matter Mater. Phys.* **2012**, *86*, 245127.
(10) Caruso, F.; Rinke, P.; Ren, X.; Scheffler, M.; Rubio, A. *Phys. Rev. B: Condens. Matter Mater. Phys.* **2012**, *86*, 081102.
(11) Körzdörfer, T.; Marom, N. *Phys. Rev. B: Condens. Matter Mater. Phys.* **2012**, *86*, 041110.
(12) Roca-Sanjuán, D.; Merchán, M.; Serrano-Andrés, L.; Rubio, M. *J. Chem. Phys.* **2008**, *129*, 095104.
(13) Trofimov, A. B.; Schirmer, J.; Kobychev, V. B.; Potts, A. W.; Holland, D. M. P.; Karlsson, L. *J. Phys. B: At., Mol. Opt. Phys.* **2006**, *39*, 305.
(14) Perdew, J. P.; Burke, K.; Ernzerhof, M. *Phys. Rev. Lett.* **1996**, *77*, 3865.
(15) Urano, S.; Yang, X.; LeBreton, P. R. *J. Mol. Struct.* **1989**, *214*, 315.
(16) Bruneval, F.; Marques, M. A. L. *J. Chem. Theory Comput.* **2013**, *9*, 324.
(17) Atalla, V.; Yoon, M.; Caruso, F.; Rinke, P.; Scheffler, M. *Phys. Rev. B: Condens. Matter Mater. Phys.* **2013**, *88*, 165122.
(18) Stan, A.; Dahlen, N. E.; van Leeuwen, R. *EPL (Europhys. Lett.)* **2006**, *76*, 298.
(19) Koval, P.; Foerster, D.; Sánchez-Portal, D. *Phys. Rev. B: Condens. Matter Mater. Phys.* **2014**, *89*, 155417.
(20) Rostgaard, C.; Jacobsen, K. W.; Thygesen, K. S. *Phys. Rev. B: Condens. Matter Mater. Phys.* **2010**, *81*, 085103.
(21) Blase, X.; Attaccalite, C.; Olevano, V. *Phys. Rev. B: Condens. Matter Mater. Phys.* **2011**, *83*, 115103.
(22) Caruso, F.; Atalla, V.; Ren, X.; Rubio, A.; Scheffler, M.; Rinke, P. *Phys. Rev. B: Condens. Matter Mater. Phys.* **2014**, *90*, 085141.
(23) Stein, T.; Kronik, L.; Baer, R. *J. Am. Chem. Soc.* **2009**, *131*, 2818.
(24) Perdew, J. P.; Zunger, A. *Phys. Rev. B: Condens. Matter Mater. Phys.* **1981**, *23*, 5048.
(25) Ruzsinszky, A.; Perdew, J. P.; Csonka, G. I.; Vydrov, O. A.; Scuseria, G. E. *J. Chem. Phys.* **2006**, *125*, 194112.
(26) Mori-Sánchez, P.; Cohen, A. J.; Yang, W. *J. Chem. Phys.* **2006**, *125*, 201102.
(27) Patchkovskii, S.; Autschbach, J.; Ziegler, T. *J. Chem. Phys.* **2001**, *115*, 26.
(28) Körzdörfer, T.; Kümmel, S.; Mundt, M. *J. Chem. Phys.* **2008**, *129*, 014110.
(29) Kümmel, S.; Kronik, L. *Rev. Mod. Phys.* **2008**, *80*, 3.
(30) Körzdörfer, T.; Kümmel, S.; Marom, N.; Kronik, L. *Phys. Rev. B: Condens. Matter Mater. Phys.* **2009**, *79*, 201205.
(31) Körzdörfer, T.; Mundt, M.; Kümmel, S. *Phys. Rev. Lett.* **2008**, *100*, 133004.
(32) Messud, J.; Dinh, P. M.; Reinhard, P.-G.; Suraud, E. *Phys. Rev. Lett.* **2008**, *101*, 096404.
(33) Pederson, M. R.; Ruzsinszky, A.; Perdew, J. P. *J. Chem. Phys.* **2014**, *140*, 121103.
(34) Stein, T.; Kronik, L.; Baer, R. *J. Chem. Phys.* **2009**, *131*, 244119.
(35) Baer, R.; Livshits, E.; Salzner, U. *Annu. Rev. Phys. Chem.* **2010**, *61*, 85.
(36) Körzdörfer, T.; Sears, J. S.; Sutton, C.; Brédas, J.-L. *J. Chem. Phys.* **2011**, *135*, 204107.
(37) Refaely-Abramson, S.; Baer, R.; Kronik, L. *Phys. Rev. B: Condens. Matter Mater. Phys.* **2011**, *84*, 075144.
(38) Karolewski, A.; Stein, T.; Baer, R.; Kümmel, S. *J. Chem. Phys.* **2011**, *134*, 151101.
(39) Stein, T.; Eisenberg, H.; Kronik, L.; Baer, R. *Phys. Rev. Lett.* **2010**, *105*, 266802.
(40) Moore, B., II; Autschbach, J. *J. Chem. Theory Comput.* **2013**, *9*, 4991.
(41) Sears, J. S.; Körzdörfer, T.; Zhang, C.-R.; Brédas, J.-L. *J. Chem. Phys.* **2011**, *135*, 151103.
(42) Körzdörfer, T.; Parrish, R. M.; Marom, N.; Sears, J. S.; Sherrill, C. D.; Brédas, J.-L. *Phys. Rev. B: Condens. Matter Mater. Phys.* **2012**, *86*, 205110.
(43) Refaely-Abramson, S.; Sharifzadeh, S.; Jain, M.; Baer, R.; Neaton, J. B.; Kronik, L. *Phys. Rev. B: Condens. Matter Mater. Phys.* **2013**, *88*, 081204.
(44) Sutton, C.; Körzdörfer, T.; Coropceanu, V.; Brédas, J.-L. *J. Phys. Chem. C* **2014**, *118*, 3925.
(45) Egger, D. A.; Weissman, S.; Refaely-Abramson, S.; Sharifzadeh, S.; Dauth, M.; Baer, R.; Kümmel, S.; Neaton, J. B.; Zojer, E.; Kronik, L. *J. Chem. Theory Comput.* **2014**, *10*, 1934.
(46) Sutton, C.; Körzdörfer, T.; Gray, M. T.; Brunsfeld, M.; Parrish, R. M.; Sherrill, C. D.; Sears, J. S.; Brédas, J.-L. *J. Chem. Phys.* **2014**, *140*, 054310.
(47) Zhang, C.-R.; Coropceanu, V.; Sears, J. S.; Brédas, J.-L. *J. Phys. Chem. C* **2014**, *118*, 154.
(48) Körzdörfer, T.; Brédas, J.-L. *Acc. Chem. Res.* **2014**, *47*, 3284.
(49) Körzdörfer, T.; Parrish, R. M.; Sears, J. S.; Sherrill, C. D.; Brédas, J.-L. *J. Chem. Phys.* **2012**, *137*, 124305.
(50) Sun, H.; Zhang, S.; Sun, Z. *Phys. Chem. Chem. Phys.* **2015**, *17*, 4337.
(51) Foster, M. E.; Wong, B. M. *J. Chem. Theory Comput.* **2012**, *8*, 2682.
(52) Agrawal, P.; Tkatchenko, A.; Kronik, L. *J. Chem. Theory Comput.* **2013**, *9*, 3473.
(53) Karolewski, A.; Kronik, L.; Kümmel, S. *J. Chem. Phys.* **2013**, *138*, 204115.
(54) Autschbach, J.; Srebro, M. *Acc. Chem. Res.* **2014**, *47*, 2592.
(55) de Queiroz, T. B.; Kümmel, S. *J. Chem. Phys.* **2014**, *141*, 084303.
(56) Sun, H.; Autschbach, J. *J. Chem. Theory Comput.* **2014**, *10*, 1035.
(57) Refaely-Abramson, S.; Sharifzadeh, S.; Govind, N.; Autschbach, J.; Neaton, J. B.; Baer, R.; Kronik, L. *Phys. Rev. Lett.* **2012**, *109*, 226405.
(58) Vydrov, O. A.; Heyd, J.; Krukau, A. V.; Scuseria, G. E. *J. Chem. Phys.* **2006**, *125*, 074106.
(59) Vydrov, O. A.; Scuseria, G. E. *J. Chem. Phys.* **2006**, *125*, 234109.
(60) Heyd, J.; Scuseria, G. E.; Ernzerhof, M. *J. Chem. Phys.* **2003**, *118*, 8207.
(61) Heyd, J.; Scuseria, G. E. *J. Chem. Phys.* **2004**, *120*, 7274.

DOI: 10.1021/acs.jctc.5b00820
J. Chem. Theory Comput. 2015, 11, 5391−5400

(62) Malagoli, M.; Coropceanu, V.; da Silva Filho, D. A.; Brédas, J. L. *J. Chem. Phys.* **2004**, *120*, 7490.
(63) Barbara, P. F.; Meyer, T. J.; Ratner, M. A. *J. Phys. Chem.* **1996**, *100*, 13148.
(64) Dierksen, M.; Grimme, S. *J. Chem. Phys.* **2004**, *120*, 3544.
(65) Santoro, F.; Improta, R.; Lami, A.; Bloino, J.; Barone, V. *J. Chem. Phys.* **2007**, *126*, 084509.
(66) Santoro, F.; Lami, A.; Improta, R.; Barone, V. *J. Chem. Phys.* **2007**, *126*, 184102.
(67) Thomas, T. D.; Saethre, L. J.; Sorensen, S. L.; Svensson, S. *J. Chem. Phys.* **1998**, *109*, 1041.
(68) Coropceanu, V.; Malagoli, M.; da Silva Filho, D. A.; Gruhn, N. E.; Bill, T. G.; Brédas, J. L. *Phys. Rev. Lett.* **2002**, *89*, 275503.
(69) Coropceanu, V.; Kwon, O.; Wex, B.; Kaafarani, B. R.; Gruhn, N. E.; Durivage, J. C.; Neckers, D. C.; Brédas, J.-L. *Chem. - Eur. J.* **2006**, *12*, 2073.
(70) Blum, V.; Gehrke, R.; Hanke, F.; Havu, P.; Havu, V.; Ren, X.; Reuter, K.; Scheffler, M. *Comput. Phys. Commun.* **2009**, *180*, 2175.
(71) Havu, V.; Blum, V.; Havu, P.; Scheffler, M. *J. Comput. Phys.* **2009**, *228*, 8367.
(72) Ren, X.; Rinke, P.; Blum, V.; Wieferink, J.; Tkatchenko, A.; Sanfilippo, A.; Reuter, K.; Scheffler, M. *New J. Phys.* **2012**, *14*, 053020.
(73) Stephens, P. J.; Devlin, F. J.; Chabalowski, C. F.; Frisch, M. J. *J. Phys. Chem.* **1994**, *98*, 11623.
(74) Shao, Y.; Gan, Z.; Epifanovsky, E.; Gilbert, A. T. B.; Wormit, M.; Kussmann, J.; Lange, A. W.; Behn, A.; Deng, J.; Feng, X.; Ghosh, D.; Goldey, M.; Horn, P. R.; Jacobson, L. D.; Kaliman, I.; Khaliullin, R. Z.; Kús, T.; Landau, A.; Liu, J.; Proynov, E. I.; Rhee, Y. M.; Richard, R. M.; Rohrdanz, M. A.; Steele, R. P.; Sundstrom, E. J.; Woodcock, H. L., III; Zimmerman, P. M.; Zuev, D.; Albrecht, B.; Alguire, E.; Austin, B.; Beran, G. J. O.; Bernard, Y. A.; Berquist, E.; Brandhorst, K.; Bravaya, K. B.; Brown, S. T.; Casanova, D.; Chang, C.-M.; Chen, Y.; Chien, S. H.; Closser, K. D.; Crittenden, D. L.; Diedenhofen, M.; DiStasio, R. A., Jr.; Dop, H.; Dutoi, A. D.; Edgar, R. G.; Fatehi, S.; Fusti-Molnar, L.; Ghysels, A.; Golubeva-Zadorozhnaya, A.; Gomes, J.; Hanson-Heine, M. W. D.; Harbach, P. H. P.; Hauser, A. W.; Hohenstein, E. G.; Holden, Z. C.; Jagau, T.-C.; Ji, H.; Kaduk, B.; Khistyaev, K.; Kim, J.; Kim, J.; King, R. A.; Klunzinger, P.; Kosenkov, D.; Kowalczyk, T.; Krauter, C. M.; Lao, K. U.; Laurent, A.; Lawler, K. V.; Levchenko, S. V.; Lin, C. Y.; Liu, F.; Livshits, E.; Lochan, R. C.; Luenser, A.; Manohar, P.; Manzer, S. F.; Mao, S.-P.; Mardirossian, N.; Marenich, A. V.; Maurer, S. A.; Mayhall, N. J.; Oana, C. M.; Olivares-Amaya, R.; O'Neill, D. P.; Parkhill, J. A.; Perrine, T. M.; Peverati, R.; Pieniazek, P. A.; Prociuk, A.; Rehn, D. R.; Rosta, E.; Russ, N. J.; Sergueev, N.; Sharada, S. M.; Sharmaa, S.; Small, D. W.; Sodt, A.; Stein, T.; Stück, D.; Su, Y.-C.; Thom, A. J. W.; Tsuchimochi, T.; Vogt, L.; Vydrov, O.; Wang, T.; Watson, M. A.; Wenzel, J.; White, A.; Williams, C. F.; Vanovschi, V.; Yeganeh, S.; Yost, S. R.; You, Z.-Q.; Zhang, I. Y.; Zhang, X.; Zhou, Y.; Brooks, B. R.; Chan, G. K. L.; Chipman, D. M.; Cramer, C. J.; Goddard, W. A., III; Gordon, M. S.; Hehre, W. J.; Klamt, A.; Schaefer, H. F., III; Schmidt, M. W.; Sherrill, C. D.; Truhlar, D. G.; Warshel, A.; Xua, X.; Aspuru-Guzik, A.; Baer, R.; Bell, A. T.; Besley, N. A.; Chai, J.-D.; Dreuw, A.; Dunietz, B. D.; Furlani, T. R.; Gwaltney, S. R.; Hsu, C.-P.; Jung, Y.; Kong, J.; Lambrecht, D. S.; Liang, W.; Ochsenfeld, C.; Rassolov, V. A.; Slipchenko, L. V.; Subotnik, J. E.; Van Voorhis, T.; Herbert, J. M.; Krylov, A. I.; Gill, P. M. W.; Head-Gordon, M. *Mol. Phys.* **2015**, *113*, 184−215.
(75) Adamo, C.; Barone, V. *J. Chem. Phys.* **1999**, *110*, 6158.
(76) Original data provided by V. Coropceanu.
(77) Sauther, J.; Wüsten, J.; Lach, S.; Ziegler, C. *J. Chem. Phys.* **2009**, *131*, 034711.
(78) Original data provided by C. Ziegler and S. Lach.
(79) Ando, N.; Mitsui, M.; Nakajima, A. *J. Chem. Phys.* **2007**, *127*, 234305.
(80) Mitsui, M.; Ando, N.; Nakajima, A. *J. Phys. Chem. A* **2007**, *111*, 9644.
(81) Crocker, L.; Wang, T.; Kebarle, P. *J. Am. Chem. Soc.* **1993**, *115*, 7818.
(82) Fu, Q.; Yang, J.; Wang, X.-B. *J. Phys. Chem. A* **2011**, *115*, 3201.
(83) Desfrancois, C.; Périquet, V.; Lyapustina, S. A.; Lippa, T. P.; Robinson, D. W.; Bowen, K. H.; Nonaka, H.; Compton, R. N. *J. Chem. Phys.* **1999**, *111*, 4569.
(84) Gallandi, L.; Marom, N.; Rinke, P.; Körzdörfer, T. *Accurate Ionization Potentials and Electron Affnities of Acceptor Molecules. II. Non-empirically Tuned Long-range Corrected Hybrid Functionals*, submitted for publication.
(85) Alves, H.; Molinari, A. S.; Xie, H.; Morpurgo, A. F. *Nat. Mater.* **2008**, *7*, 574.
(86) Beljonne, D.; Cornil, J.; Muccioli, L.; Zannoni, C.; Brédas, J.-L.; Castet, F. *Chem. Mater.* **2011**, *23*, 591.
(87) Wen, S.; Deng, W.-Q.; Han, K.-L. *Chem. Commun.* **2010**, *46*, 5133.
(88) Beltrán, J. I.; Flores, F.; Martinez, J. I.; Ortega, J. *J. Phys. Chem. C* **2013**, *117*, 3888.
(89) Sini, G.; Sears, J. S.; Brédas, J.-L. *J. Chem. Theory Comput.* **2011**, *7*, 602.

DOI: 10.1021/acs.jctc.5b00820
J. Chem. Theory Comput. 2015, 11, 5391−5400